NJC

Accepted Manuscript

This is an *Accepted Manuscript*, which has been through the Royal Society of Chemistry peer review process and has been accepted for publication.

Accepted Manuscripts are published online shortly after acceptance, before technical editing, formatting and proof reading. Using this free service, authors can make their results available to the community, in citable form, before we publish the edited article. We will replace this *Accepted Manuscript* with the edited and formatted *Advance Article* as soon as it is available.

You can find more information about *Accepted Manuscripts* in the Information for Authors.

Please note that technical editing may introduce minor changes to the text and/or graphics, which may alter content. The journal's standard Terms & Conditions and the Ethical guidelines still apply. In no event shall the Royal Society of Chemistry be held responsible for any errors or omissions in this *Accepted Manuscript* or any consequences arising from the use of any information it contains.

ROYAL SOCIETY OF CHEMISTRY

www.rsc.org/njc

Facile synthesis of biocompatible silver nanoparticle derived tripeptide supramolecular hydrogel for antibacterial wound dressings

Turibius Simon, Chung-Shu Wu, Jie-Chuan Liang, Chieh Cheng, and Fu-Hsiang Ko*

Department of Materials Science and Engineering,

National Chiao Tung University, 1001 University Road, Hsinchu, Taiwan 300, ROC

Corresponding author: fhko@mail.nctu.edu.tw (+886-35712121 ext 55803)

Abstract

Realizing the widespread demand of biocompatible supramolecular hydrogel based wound dressings, we have developed a N-terminally 2-(Naphthalen-6-yl) acetic acid (Nap) protected Phe-Phe-Cys peptide (Nap-FFC) by liquid phase method. This Nap-FFC peptide was used to design supramolecular hydrogel via self-assembling process. The Nap-FFC short peptides produced stable and transparent silver nanoparticle-based hydrogels (AgNPs@Nap-FFC) wherein the self-assembled Nap-FFC nanofibers acted as scaffolds for the mineralization of silver nanoparticles (AgNPs) and stabilizer of synthesized AgNPs. The resultant AgNPs@Nap-FFC nanocomposites were characterized by ultraviolet-visible spectrophotometry (UV-vis spectroscopy), Fourier transform infrared spectroscopy (FT-IR), Transmission electron microscopy (TEM) and Scanning electron microscopy (SEM) equipped with energy-dispersive X-ray spectroscopy (EDX) studies. The AgNPs@Nap-FFC nanocomposites showed excellent monodispersity, long term stability, and functional flexibility in comparison to other AgNPs based nanocomposites. Furthermore, AgNPs@Nap-FFC exhibited strong inhibition against both Gram-positive (Methicillin-resistant *Staphylococcus aureus*) and Gram-negative (*Acinetobacter baumannii*) bacteria and, most importantly they showed favorable biocompatibility towards human cervical carcinoma cells (HeLa cells). Hence, this study implies that AgNPs@Nap-FFC nanocomposites can easily be prepared in a cost-effective manner and can be used effectively for future antibacterial wound dressings.

Introduction

Much attention has been devoted to the pharmacology of silver nanoparticles (AgNPs) in terms of their large surface area to volume ratio, physicochemical properties, antioxidant activities and low toxicity to mammalian cells.[1-3] The AgNPs induces the production of hydroxyl radicals (•OH) to kill bacterial cells, without interacting with the multidrug-resistant pumps in bacteria that produce toxins to inhibit antibiotics like ampicillin. This suggests that resistance to AgNPs particles is less likely to occur in bacteria and hence it can be used as a new generation antimicrobial agent to overcome the drug resistance seen with Gram-negative and Gram positive bacteria.[4,5] This unique character enabled AgNPs to be used in a wide variety of products such as refrigerators, clothes, toothbrushes, and cosmetics.[6] The AgNPs has been shown to have superior cytotoxicity against a wide range of microorganism when compared to many metal nanoparticles.[7] However, bare AgNPs (e.g. sodium borohydride/citrate reduced AgNPs) are unstable in aqueous medium, due to the release of surface bound Ag^+ ion thereby, causing the loss of antibacterial activity and inducing cellular toxicity and reactive oxygen species (ROS) production to normal cells upon over time exposure.[8,9] Hence there is a need to synthesize stable biocompatible AgNPs in order to reduce their cellular toxicity in health care or biomedical applications.[10,11] Different polymer nanocomposites such as poly (oxyethylene)-segmented imide (POEM), poly (styrene-co-maleic anhydride)-grafting poly (oxyalkylene) (SMA) and poly (vinyl alcohol) (PVA) have been employed to stabilize AgNPs and been used for biomedical applications.[12] But, the stabilization of polymer based nanocomposite materials requires prolonged synthesis steps, high cost, and show inadequate biocompatibility.[13]

To improve the biocompatibility and to shorten the synthesis steps, proteins or artificial self-assembling peptide-based scaffolds are employed to synthesis peptide based nanocomposite materials through biomineralization mechanism.[14] Common biomimetic peptides include fibronectin-derived RGDS sequence for therapeutic cell delivery[15], the laminin derived IKVAV sequence[16] used for bone regeneration and wound healing etc. In addition, self-assembled peptide-based hydrogels could be used for various therapeutic approaches such as; for the regeneration of enamel, cartilage, and the central nervous system, as well as delivery vehicles, transplantation of islets, wound-healing and cardiovascular therapies.[17,18] Among self-assembling peptides used[19], diphenylalanine (FF) peptide and its derivatives can be more easily self-assembled into various nanostructures than other lengthy peptides applied for biomedical applications.[20] Proceeding from these research reports, we decided to introduce an efficient peptide-tunable hydrogel, co-fabricated with AgNPs. Accordingly, an N-terminally protected FF peptide derivative (Nap-FFC) was synthesized in laboratory-scale, which showed robust metal binding ability with AgNPs and was able to form stable and transparent AgNPs@Nap-FFC hydrogels. The synthetic reactions were mild and environment friendly. Further, bioassays revealed that the synthesized AgNPs@Nap-FFC nanocomposites possess an effective and long term antibacterial activity against both Gram–positive bacteria and Gram–negative bacteria. Most importantly, the AgNPs@Nap-FFC hydrogels were proven to be non-toxic to human cells, and therefore this approach would be a versatile platform in the mechanobiology. Due to the strong bacterial inhibition activities, this novel AgNPs@Nap-FFC hydrogels could be an attractive antibacterial material for use as wound dressings in biomedical applications.

Materials and methods

Chemicals and reagents

2-(Naphthalen-6-yl) acetic acid (Nap), N,N'-Dicylcohexylcarbodiimide (DCC), N-hydroxysuccinimide (NHS), L-phenylalanine (Phe), L- Cystein (Cys) and sodium carbonate (Na_2CO_3) were purchased from Alfa Aesar and used without further purification. Silver nitrate ($AgNO_3$), sodium borohydride ($NaBH_4$), chloroform ($CHCl_3$) and methanol (CH_3OH) were obtained from Aldrich, U.S.A. Metal salts such as $ZnCl_2$, $MgCl_2$, $AgCl_2$, $FeCl_2$, $CoCl_2$, $CdCl_2$, $BaCl_2$, LiCl, $NiCl_2$, KCl and $CaCl_2$ were from Baker Analyzed ACS Reagent, U.S.A. Bacterial strains (Methicillin-resistant Staphylococcus aureus and Acinetobacter baumannii) and HeLa cell lines were from BCRC (Bioresource Collection and Research Center) Taiwan. Bacterial culture media such as trypticase soy broth (TSB) and trypticase soy agar (TSA) were, purchased from Becton, Dickinson and Company. The medium used for the culture of HeLa cells was Dulbecco's modified eagle medium (DMEM-Thermo Scientific).

Instruments and product characterizations

Molecular structures of Nap-F, Nap-FF, and Nap-FFC were elucidated by Nuclear magnetic resonance (NMR, Bruker 300MHz spectrometer) and High resolution mass analysis (HRMS, Waters Premier XE instrument with ESI source). The ionic interactions of Nap-FFC with various metal ions were determined using Fourier transform infrared spectroscopy (FTIR, Perkin Elmer spectrometer 100 FT-IR SPECTRUM ONE) and compared deduced reactions. The silver nanoparticles (AgNPs) and silver based Nap-FFC nanocomposites (AgNPs@Nap-FFC) were characterized by UV-Vis spectroscopy

(HITACHI, U-3310), Scanning electron microscope (SEM, JEOL, JSM-6700) and Transmission electron microscopy (TEM, JEOL, JEM-2100).

Synthesis of biocompatible Peptide:

N-terminally Nap protected peptide Nap-FFC (Nap-Phe-Phe-Cys) was synthesized using liquid phase method.[21]

Synthesis of Nap-F

2-(Naphthalen-6-yl) acetic acid (Nap, 372 mg, 2 mmol) and N-hydroxysuccinimide (NHS, 230 mg, 2 mmol) were dissolved in 20 mL chloroform and N,N'-Dicylcohexylcarbodiimide (DCC, 432 mg, 2.1 mmol) was added. The mixture was stirred at room temperature for 5hr, then the resulting solid was filtered off, and the filtrate was subjected to rotary evaporation. The crude product obtained (Nap-NHS) was used without purification. L-Phenylalanine (330 mg, 2mmol) and sodium carbonate (Na_2CO_3, 424 mg, 4 mmol) were dissolved in 8 mL of water, the solution of the crude product (Nap-NHS) (dissolved in 20 mL acetone) was added, and the resulting reaction mixture was stirred at room temperature overnight. The reaction mixture was subjected to rotary evaporation, and then 20 mL of water was added. The filtrate was acidified to pH 3 and the resulting product obtained by filtration was further purified by flash column with chloroform-methanol as the eluent. Compound Nap-F (white powder) was collected with 58% yield. 1H NMR (300 MHz, DMSO-d6) δ(ppm): 8.44 (d, J = 8.1Hz, 1NH), 7.86-7.75 (m, 3H), 7.64 (s, 1H), 7.46 (t, J = 6Hz, 2H), 7.27-7.18 (m, 6H), 4.42(t, J = 4.2Hz, 1H), 3.57 (d, 2H), 3.09-2.82 (m, 2H). HRMS (ESI-): Calculated for $C_{21}H_{19}NO_3$ 333.1365 found [M-H]- 332.1281.

Synthesis of Nap-FF

Compound Nap-F (333 mg, 1 mmol) and NHS (115 mg, 1 mmol) were dissolved in chloroform (10 mL) and DCC (216 mg, 1.05 mmol) was added. The mixture was stirred at room temperature for 5 hr, then the resulting solid was filtered off, and the filtrate was subjected to rotary evaporation. The crude product obtained (Nap-F-NHS) was used without purification. L-Phenylalanine (165 mg, 1 mmol) and Na_2CO_3 (212 mg, 2 mmol) were dissolved in 4 mL of water, the solution of crude product (Nap-F-NHS) was dissolved in 10 mL of acetone, and then the resulting reaction mixture was stirred at room temperature overnight. The reaction mixture was subjected to rotary evaporation, and then 10 mL of water was added. The filtrate was acidified to pH 3, and the resulting product obtained by filtration was further purified by flash column with chloroform-methanol as the eluent. The dipeptide Nap-FF (white powder) was collected with 50% yield. 1H NMR (300 MHz, DMSO-d6) δ (ppm): 8.29-8.49 (m, 3H), 7.42-7.86 (m, 3H), 7.10-7.28(m, 8H), 4.44-4.59 (m, 2H, -CH), 2.95-3.10 (m, 3H), 2.68-2.92 (m, 3H). HRMS (ESI-): Calculated for $C_{30}H_{28}N_2O_4$ 480.2049 found [M-H]- 479.1966.

Synthesis of Nap-FFC

Compound Nap-FF (240 mg, 0.5 mmol) and NHS (57.5 mg, 0.5 mmol) were dissolved in chloroform (6 mL) and DCC (107 mg, 0.52 mmol) was added. The mixture was stirred at room temperature for 5 hr, then the resulting solid was filtered off, and the filtrate was subjected to rotary evaporation. The crude product obtained (Nap-FF-NHS) was used without purification. L-Cysteine (60.5 mg, 0.5 mmol) and Na_2CO_3 (106 mg, 1 mmol) were dissolved in 2 mL of water; the solution of crude product (Nap-FF-NHS) dissolved in 6 mL of acetone was added. And the resulting reaction mixture was stirred at

room temperature overnight. The reaction mixture was subjected to rotary evaporation, and then 10 mL of water was added. The filtrate was acidified to pH 3 and the resulting product obtained by filtration was further purified by flash column with chloroform-methanol as the eluent. The final compound Nap-FFC (white powder) was collected with 30% yield. The 1H NMR (300 MHz, DMSO-d6) δ (ppm): 12.93[s (br), 1H (-COOH)], 8.25-8.48 [m, 6H (–NH & aromatic)] 7.30-7.48 [m, 3H, (aromatic)], 7.10-7.24 [m,8H (aromatic)], 4.44-4.59 [m,3H(-CH)], 2.95-3.09 [m,4H (-CH2)], 2.50-2.84 [m, 4H(-CH2)], 1.761[s (br),1H (SH)]. HRMS (ESI-): Calculated for $C_{33}H_{33}N_3O_5S$ 583.2141 found [M-H]- 582.2070.

Gelation properties of the Nap-FFC

Different concentrations of Nap-FFC (w/v) in aqueous solution at different pH condition were, evaluated for their gelation properties.

Synthesis of silver nanoparticles (AgNPs)

62.5 µL of 0.1 M silver nitrate (AgNO3) and freshly prepared ice cold 300 µL of 5 mM sodium borohydride ($NaBH_4$) were added in 25 mL of distilled water with continuous stirring. The reaction was carried out in room temperature for 30 minutes. The reaction mixture slowly turned to yellow coloured solution, indicating the formation of AgNPs.[22] The prepared AgNPs solution was stored at 4^oC for further study.

Synthesis of AgNPs@Nap-FFC nanocomposites

62.5 µL of 0.1 M Silver nitrate ($AgNO_3$) was added in 25 mL of 120 µM Nap-FFC solution (pH 12). The mixture was gently stirred for 30 minutes at room temperature. Then, freshly prepared cold 300 µL of 5 mM sodium borohydride ($NaBH_4$) was added to the reaction mixture. The reaction mixture then slowly turned to brown

colour solution, indicating the formation of silver nanoparticle based Nap-FFC nanocomposites (AgNPs@Nap-FFC).

Antibacterial activity determination

The antibacterial activity of AgNPs@Nap-FFC hydrogel was evaluated by direct contact with gram positive and gram negative bacteria. The common drug resistant bacterial strains such as Methicillin-resistant *Staphylococcus aureus* and *Acinetobacter baumannii* were tested. In brief, bacterial strains cultured in 2 mL of trypticase soy broth (TSB) were treated with AgNPs@Nap-FFC hydrogel at a concentration of 40 and 80 μg/mL of bacterial medium. Bacterial growth rates were determined by measuring the optical density (OD) at 600 nm using a spectrophotometer (Cell density meter). For the bactericidal activity assay, bacteria were grown on TSA plates at 37 °C for 24 hours to obtain the late-log growth phase (OD_{600} = 2.0). The plates were incubated with 1% (w/v) Nap-FFC hydrogel pad and AgNPs@Nap-FFC nanocomposites (80 μg/mL). Meanwhile, 1% Nap-FFC (w/v) hydrogel pad incubated under the same environments was used as a control. The agar plates were incubated at room temperature and the bacterial growth rates were determined by measuring the OD at 600 nm.

Biocompatibility studies by MTT assay

In order to evaluate the cytotoxic activity of AgNPs@Nap-FFC nanocomposites, human cervical carcinoma (HeLa) cells were used in this study. HeLa cells were maintained in Dulbecco's modified Eagle's medium (DMEM) supplemented with 10% fetal bovine serum (FBS) and 1X antibiotics solution, and cultured at 37° C in a humidified incubator containing 5% CO_2. For cytotoxicity assay, cells were grown in 96-well plates (flat bottom) at a density of 1.5×10^4 cells/well with 100 μL of medium. After

overnight culturing, the culture medium was aspirated and fresh media containing AgNPs@Nap-FFC nanocomposites at concentrations ranging from 10 to100 µg/mL was added and incubated for 24 h. Inorder to determine the viability of HeLa cells, 100µl of MTT solution (5 mg/mL) diluted in serum free DMEM medium was added, and incubated at 37° C for 4 h. After 4 hrs of incubation purple colored crystals formed were dissolved in DMSO and the absorbance was measured at 570 nm using a Multiskan GO micoplate reader. All experiments were independently performed for at least three times. The results were presented as percentage of viable cells against increasing dose of AgNPs@Nap-FFC nanocomposites. The untreated cells served as control.

Results and discussion

Physicochemical characterization of Nap-FFC peptides

The preparation method of Nap protected FFC peptide (Nap-Phe-Phe-Cys) via liquid phase approach is illustrated in Fig. S1.The primary molecular structure of Nap-F, Nap-FF, and Nap-FFC were confirmed by NMR spectra of each compound (Fig. S2-S4). The molecular structures of synthesized peptides, Nap-F, Nap-FF, and Nap-FFC were further verified by high resolution mass analysis (Fig. S5-S7). The data obtained from NMR and high resolution mass spectra revealed the exact peptide sequence identity peak and mass value of those compounds. The Supramolecular Nap-FFC peptide structure showed two different moieties: hydrophobic and hydrophilic. The hydrophobic group promotes self-assembling process to form hydrogels. On the other hand, the hydrophilic moiety exhibits many carboxylic acid and thiol groups on the supramolecule nanofibers (Nap-FFC) surface, which can act as silver metal ion binding sites and nucleation sites for the growth of silver nanoparticles. The synthesized, Nap-FFC peptide has free

carboxylic acid and thiol groups which enable to tune the peptide nature based on desired conditions. These peptides can self-assemble to form supramolecular hydrogel with respect to different conditions, such as the peptide weight percentage concentration (w/v), pH condition and mineralisation with metal ions. For this study, we have taken Nap moiety as a protecting group since it is present in clinically approved drug molecules such as Propranolol and Naphazoline, and are more biocompatible than Fmoc or Pyrene groups.[23] The hydrophilic moiety of Nap-FFC has numerous carboxylic acid and thiol groups in the peptide nanofibers surface, which acts as a nucleation sites for the growth of nanoparticle and metal binding sites, respectively. The mineralization process of silver ion by peptide nanofibers are shown in Fig. 1. We proposed the synthetic method of supramolecular AgNPs entrapped hydrogel (AgNPs@Nap-FFC) nanocomposites. The above mechanism favours more advantage than other methods due to ease of fabrication, good biocompatibility, cost effectiveness, acceleration of wound healing process, molecular recognition capability and functional flexibility.[2,24] The metal ions can coordinate with negatively charged carboxylic acid groups and thiol group through electrostatic interaction process and are reduced to metal atoms. The Ag ions were able to coordinate more effectively with Nap-FFC and henceforth we used sodium borohydride which subsequently initiate the generation of Ag nuclei that finally grow into AgNPs along with peptide nanofibers. This mechanism of bio-mineralisation enabled to prepare the silver nanoparticle based Nap-FFC nanocomposites (AgNPs@Nap-FFC).

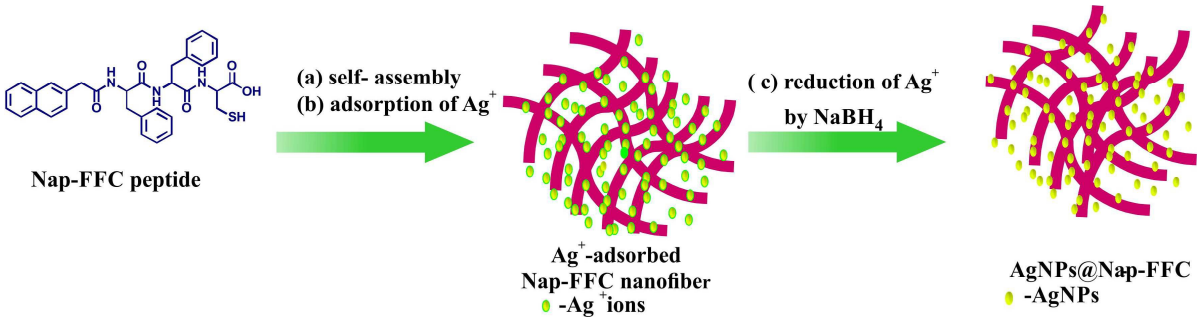

Figure 1. Schematic illustration for the preparation process of AgNPs@Nap-FFC nanocomposites.

Gelation property of Nap-FFC

Different pH induced phase transition of 1% Nap-FFC hydrogel (w/v) at 30°C are shown in Fig. 2. The 1% w/v Nap-FFC was completely soluble at pH >10, due to the stable deprotonation of the compound at highly alkali condition. Interestingly, Nap-FFC hydrogel (1% w/v) was semi-transparent at pH ranging from 7 to 10, but in acidic pH range (5 to 6) the hydrogel was opaque. In addition, at low pH (pH= 4) the 1% (w/v) Nap-FFC hydrogel was starting to form precipitate, which might be because of stable protonation. The formation of hydrogel within a narrow pH range (5 to 6) likely arises from a balance of protonation/deprotonation of the C-terminal carboxyl group.[25-27]

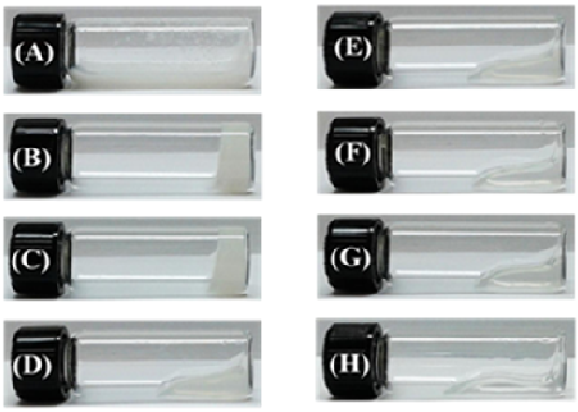

Figure 2. Optical images of Nap-FFC hydrogel ([Nap-FFC] = 1 wt %). Nap-FFC hydrogel (1 wt %) exists as (A) a precipitates at pH < 4.0, (B and C) a strong opaque hydrogel at pH ranges of about 4.0 to 6.0, (D, E, F and G) a weak transparent hydrogel at pH ranges of about 7.0 to 10.0, and (H) a clear solution at pH >10.

FT-IR analysis

The interaction of Nap-FFC peptide with silver ions was studied using FT-IR analysis, as shown in Fig. S8. The IR peak indicates the presence of C=O groups at 1670 cm^{-1} and the S–H stretching of Nap-FFC at 2569cm^{-1}.[28] Interestingly, the S–H and C=O stretching bands at 2569, 1670cm^{-1} of Nap-FFC were absent due to the binding of silver ions to carbonyl and thiol terminal of Nap-FFC. According to the above results, the Nap-FFC peptide displayed a carboxylic acid and thiol group on the supramolecule nanofibers surface, which offer the strong interaction with silver ions.[29,30]

Stability of AgNPs@Nap-FFC nanocomposite

To examine the stability, Nap-FFC peptide nanocomposites (AgNPs@Nap-FFC) produced via in situ reduction method was compared with bare AgNPs (NaBH4 reduced) by UV-Vis absorption spectrum. The UV-vis absorption spectrum of the bare AgNPs and AgNPs@Nap-FFC shows a surface plasmon resonance (SPR) absorption peak at 400 nm and 420 nm respectively, as shown in Fig. 3 (A) and (B). The characteristic SPR peaks of bare AgNPs at 400 nm showed large decrements in absorption intensity within seven days due to the serious aggregation of AgNPs that usually leads to significant decrease of antibacterial effect. The SPR band of AgNPs@Nap-FFC nanocomposites is somewhat longer than that of typical bare AgNPs and this red-shift in wavelength is due to the high

dielectric constant of Nap-FFC peptide, which lowers the plasmon frequency.[31,32] On the other hand, the UV-vis spectra of AgNPs@Nap-FFC nanocomposites showed only a slight change in shifting of SPR band (~2 nm) over a time period of 30 days. Thus, the AgNPs@Nap-FFC peptide nanocomposites specify long term high stability. Furthermore, the morphologies of bare AgNPs and AgNPs@Nap-FFC peptide nanocomposites were examined by SEM analysis and images are shown in Fig. 3 (C) and (D), respectively. The average size of bare AgNPs and mineralised AgNPs obtained from Nap-FFC nanofibers are approximately ~ 15 nm and ~ 10 nm respectively. The TEM analysis further confirms the size of AgNPs and AgNPs@Nap-FFC peptide nanocomposites (shown in Fig. S9). Therefore, the newly developed AgNPs@Nap-FFC peptide nanocomposite has a high monodispersity and long term stability even in aqueous medium.

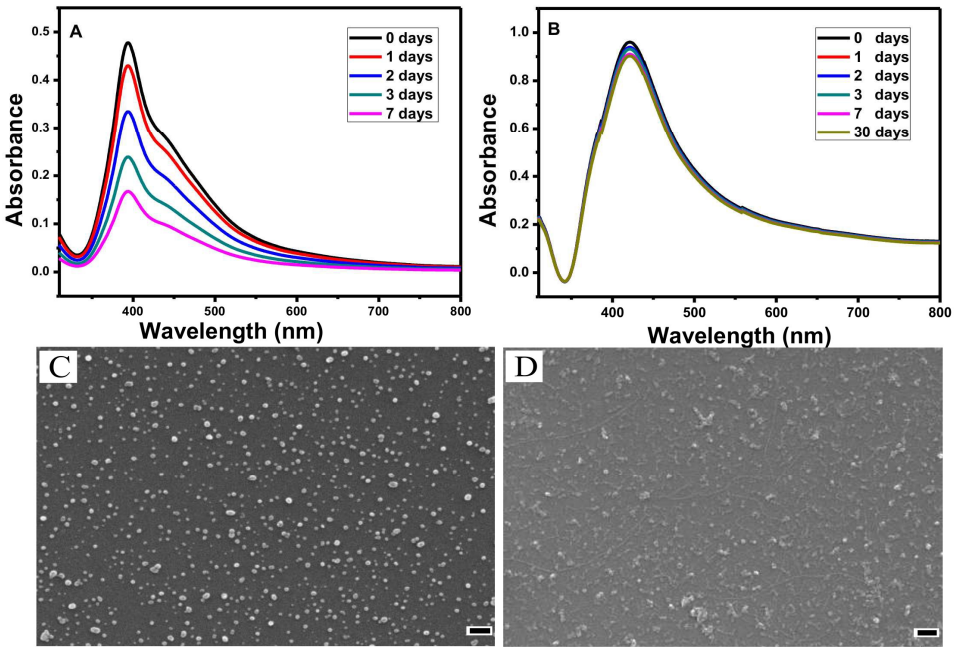

Figure 3. The absorption spectra and SEM analysis of AgNPs (A, C) and AgNPs@Nap-FFC nanocomposite (B, D) at pH-7.4. Scale bar: 100nm.

For antibacterial application, the hydrogel was formed by combining 80 µg/mL AgNPs@Nap-FFC peptide nanocomposites (liquid form) with 1 % Nap-FFC (no AgNPs present) at pH 12. Also, the effect of gelation of AgNPs@Nap-FFC was systematically studied at different period (shown in Fig. S10). According to the photographic images, the time dependent gelation can be seen when 80 µg/mL of AgNPs@Nap-FFC was added to 1 % Nap-FFC which was able to form hydrogels overnight. No characteristic gelations were seen at 30 min even in the presence of AgNPs@Nap-FFC but hydrogel formation was observed after overnight incubation, due to the self-assembly process of Nap-FFC, with respect to time. On the contrary, we also observe that clear solution of 1 % Nap-FFC (w/v) without AgNPs@Nap-FFC doesn't change phase after overnight time period. The SEM image (Fig.4a,b), ensured the morphology of the 1 % (w/v) Nap-FFC with/without AgNPs@Nap-FFC nanocomposites (80 µg/mL) and we noticed the uniform dispersion of AgNPs on the surface of the Nap-FFC nanofiber. Further confirmation of the presence AgNPs in NapFFC nanocomposites was done by EDX analysis (Fig.4c). The peak in EDX spectra indicates the presence of silver at 3 KeV and the C and O peak at 0.2 and 0.4 KeV, respectively, which is related to the amino acid of Nap-FFC.

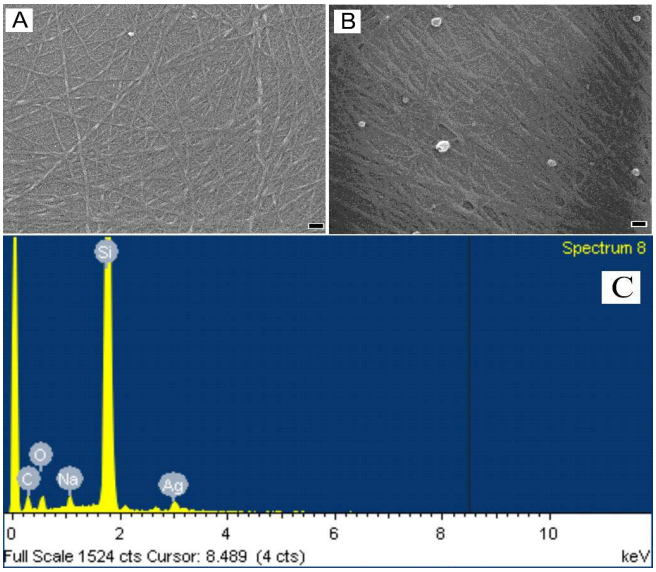

Figure 4. The SEM analysis (A and B) of 1 % (w/v) Nap-FFC without/with 80 µg/mL AgNPs@Nap-FFC. The EDX analysis (C) of 1 % (w/v) Nap-FFC containing 80 µg/mL AgNPs@Nap-FFC. Scale bar: 100nm.

Bacterial kinetic test

Bacterial kinetic test was performed to determine the antibacterial activity of Nap-FFC and AgNPs@Nap-FFC nanocomposites. As shown in Fig. 5, comparison of the growth curves of the control bacteria, to the test bacteria shows that, Nap-FFC at 120 µM, did not alter the growths of *S. aureus* and *A. baumannii*, suggesting that it has no inhibitory effect on these bacteria (Fig. 5a,c). On the other hand, even 40 µg/mL of AgNPs@Nap-FFC was able to slow down the growth of both *S. aureus* and *A. baumannii* at 12 and 28 hrs respectively. Moreover, when the concentration of AgNPs@Nap-FFC was increased to 80 µg/mL (Fig. 5b,d), the growth of both bacteria showed strong long-term inhibition revealing that, these nanocomposites can be an attractive biomaterial for applications such as wound dressing.

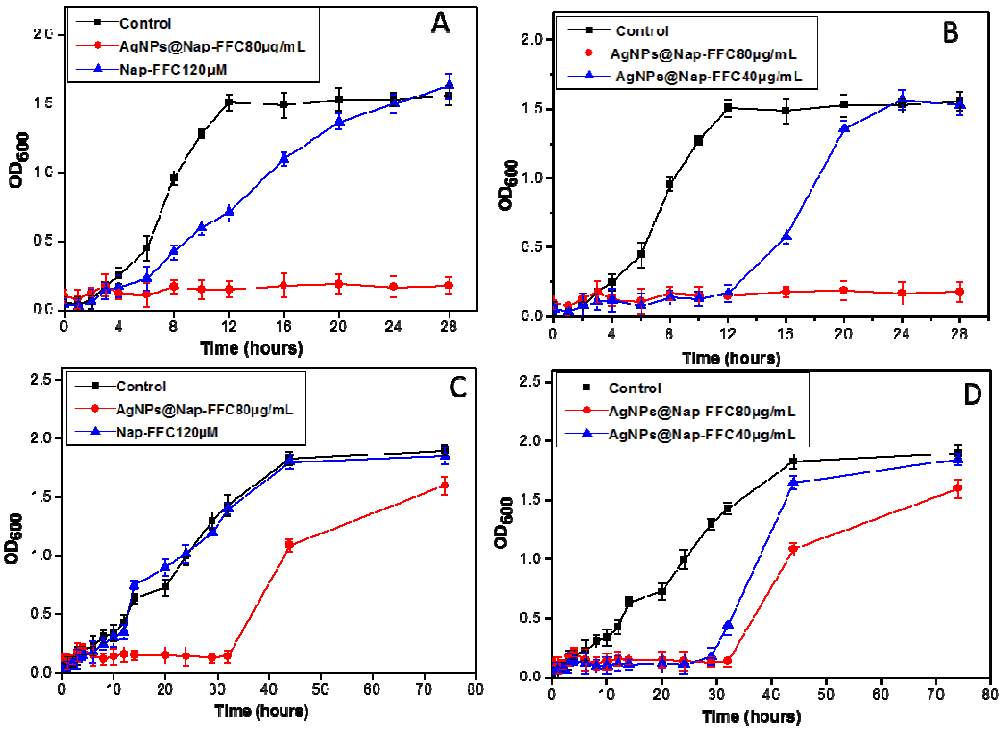

Figure 5. Bacterial growth curves in Luria-Bertani (LB) media with Nap-FFC or AgNPs@Nap-FFC nanocomposites stored at 4^0C for 7 days. Comparison of the antibacterial activity of Nap-FFC and AgNPs@Nap-FFC against Methicillin-resistant *Staphylococcus aureus* (A and B) and *Acinetobacter baumannii* (C and D).

Bacterial spread plate method

The antibacterial activity of the Nap-FFC and AgNPs@Nap-FFC nanocomposites were further ensured by bacterial spread plate method. For this, Nap-FFC without/with AgNPs@Nap-FFC respectively were layered over a lawn of *S. aureus* and *A. baumannii* in a TSA plate, and incubated at room temperature for 12 and 24 hours. After 12 hours of incubation, only the AgNPs@Nap-FFC (80 µg/mL) produced a clearly visible area of inhibition (Fig. 6 and 7), suggesting excellent bacterial inhibition property due to the release of large amount of nanosilver particles (Fig. 6 and 7). The antibacterial activity

was maximum and then decreased after 24 hours of incubation due to gradual decrease in the amount of nanosilver particles released, which was also reported in the previous studies.[33] Henceforth, resumed growth of both bacteria occurred when the concentration of nanosilver decreased below the minimum inhibitory concentration. So, we speculate that under different time phases, the decreasing nanosilver concentration may result in lower antibacterial activity.

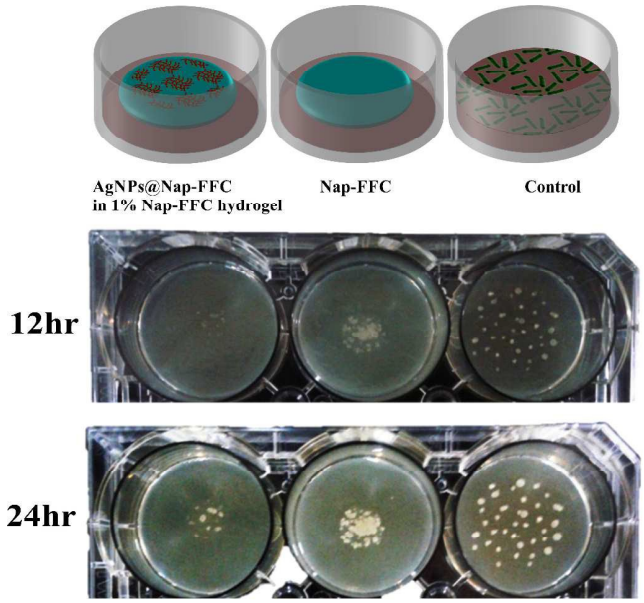

Figure 6. (a) Schematic illustration of the antibacterial test of Nap-FFC and AgNPs@Nap-FFC hydrogels. (b) Petri plates with Luria-Bertani (LB)-agar inoculated with Methicillin-resistant *staphylococcus aureus,* showing variable numbers of colonies when supplemented 1 % (w/v) Nap-FFC with/without 80 µg/mL AgNPs@Nap-FFC.

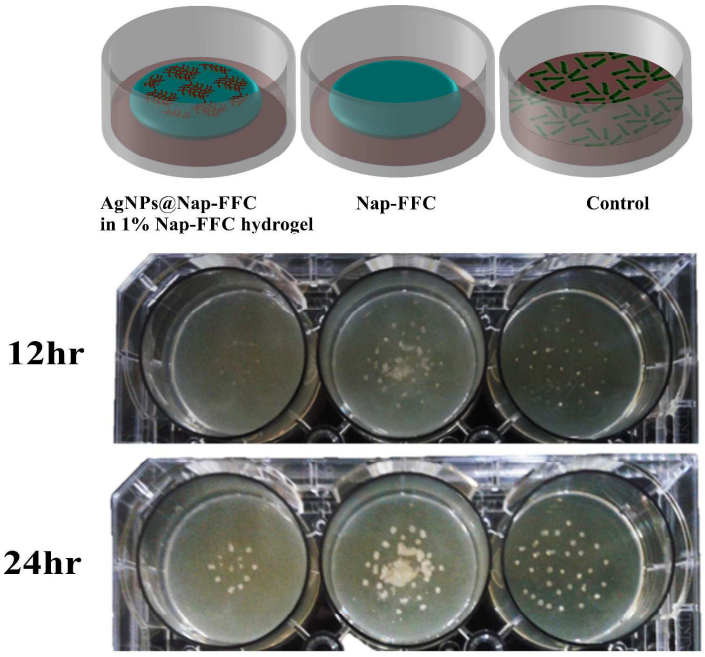

Figure 7. (a) Schematic illustration of the antibacterial test of Nap-FFC and AgNPs@Nap-FFC hydrogels. (b) Petri plates with Luria-Bertani (LB)-agar inoculated with *Acinetobacter baumannii*, showing variable numbers of colonies when supplemented 1 % (w/v) Nap-FFC with/without 80 μg/mL AgNPs@Nap-FFC.

Biocompatibility of AgNPs@Nap-FFC nanocomposites

To further test the potential application of AgNPs@Nap-FFC nanocomposites, we evaluated the toxic effects of these nanocomposites in human HeLa cells by MTT assay. After 24 hours of incubations, we found that the AgNPs@Nap-FFC nanocomposites showed no or little effect on HeLa cells at concentrations upto 80 μg mL^{-1}(Fig. 8). Even though increasing the concentration of AgNPs@Nap-FFC nanocomposite upto 100 μg mL^{-1}, they display only mild decrease in human cell viability ensuring its less cytotoxicity and proving to reduce the risk of harmful side effects. Moreover, Nap moiety adopted to prepare this peptide has been used in clinically approved drug molecules such

as Propranolol and Naphazoline,[23] which adds more safety nature of this nanocomposites. The supramolecular hydrogel can provide the moisture environment to enhance the human cell growth. Overall, 80–90% cells were found to be viable at 40, 80 μg mL^{-1} of AgNPs@Nap-FFC nanocomposites. These data suggested that the AgNPs@Nap-FFC nanocomposite has favourable biocompatibility towards human cells.

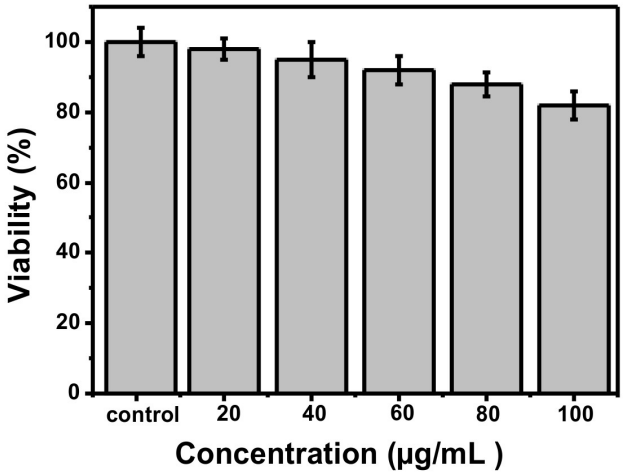

Figure 8. Cytotoxicity assay of AgNPs@Nap-FFC nanocomposites at pH-7.4 . The viability of HeLa cells incubated with different concentrations (20, 40, 60, 80, 100 μg/mL) of AgNPs@Nap-FFC nanocomposites for 24 h. Each data point represents the mean values from at least three independent experiment.

Conclusions

In summary, we report the synthesis of Nap-FFC peptide based nanofibers which were utilized to produce AgNPs@Nap-FFC nanocomposites via mineralization process. After the successful synthesis, Nap-FFC and AgNPs@Nap-FFC were characterized by NMR, high resolution mass analysis, SEM, TEM, FTIR and EDX. This silver based nanocomposite (AgNPs@Nap-FFC) offered an extended stability of approximately 30

days than that of bare AgNPs ($NaBH_4$ reduced). Also, the factors which influence the formation of hydrogel such as, effect of gelation at different pH and mineralization of Nap-FFC peptide with various metal ions were systematically studied. Results revealed that the interaction of Nap-FFC peptides with Ag^+ ion was more pronounced due to the presence of carboxyl and thiol group in Nap-FFC resulting in the formation of AgNPs@Nap-FFC. The optimum condition to prepare AgNPs@Nap-FFC is, 1% Nap-FFC (w/v) in pH 12 at 30° C. For antibacterial study, a hydrogel pad was prepared by mixing AgNPs@Nap-FFC (80 μg/mL) in 1 % Nap-FFC (w/v) peptide. These nanocomposite pads showed strong antibacterial effect against both Gram-positive and Gram-negative bacteria. Moreover, the nanocomposites displayed significant biocompatibility towards HeLa cells. Therefore, the prepared AgNPs@Nap-FFC peptide nanocomposites are promising candidates of antibacterial soft material for future tissue engineering and wound dressing.

Acknowledgements

The authors are grateful to the National Taiwan University Hospital Hsinchu Branch and the Ministry of Science and Technology of Taiwan for financially supporting this research under the contract MOST 101-2113-M-009-007-MY3.

References

1 S. Ninganagouda, V. Rathod, D. Singh, J. Hiremath, A. K. Singh, J. Mathew and M. ul-Haq, *BioMed. Res. Int*., 2014, **2014**, 9; (b) L. Liu, J. Liu, Y. Wang, X. Yan and D. D. Sun, *New J. Chem*., 2011, **35**, 1418.

2 Y. Wang, L. Cao, S. Guan, G. Shi, Q. Luo, L. Miao, I. Thistlethwaite, Z. Huang, J. Xu and J. Liu, *J. Mater. Chem*., 2012, **22**, 2575.

3 S. Agnihotri, G. Bajaj, S. Mukherji and S. Mukherji, *Nanoscale*, 2015, **7**, 7415; (b) S. Agnihotri, S. Mukherji and S. Mukherji, *RSC Adv*., 2014, **4**, 3974.

4 Y. Zhou, M. Kogiso, M. Asakawa, S. Dong, R. Kiyama and T. Shimizu, *Adv. Mater*., 2009, **21**, 1742; (b) S. Pal, Y. K. Tak, E. Han, S. Rangasamy and J. M. Song, *New J. Chem.*, 2014, **38**, 3889.

5 S. Gurunathan, J. W. Han, D. N. Kwon and J. H. Kim, *Nanoscale Res. Lett*., 2014, **9**, 373; (b) A. Chowdhuri, S. Tripathy, C. Haldar, B. Das, S. Roy and S.K. Sahu, *RSC Adv*., 2015, **5**, 21515.

6 S. Chernousova and M. Epple, *Angew. Chem. Int. Ed*., 2013, **52**, 1636; (b) L. Shahriary, R. Nair, S. Sabharwal and A. A. Athawale, *New J Chem*., 2015, **39**, 4583.

7 A. Shome, S. Duta, S. Maiti and P.K. Das, *Soft Matter*, 2011,**7**, 3011.

8 M. Lv, S. Su, Y. He, Q. Huang, W. Hu, D. Li, C. Fan and S. T. Lee, *Adv. Mater*., 2010, **22**, 5463.

9 M. Auffan, J. Rose, M. R. Wiesner and J. Y. Bottero, *Environ. Pollut*., 2009, **157**, 1127.

10 Y. Cheng, L. Yin, S. Lin, M. Wiesner, E. Bernhardt and J. Liu, *J. Phys. Chem. C*, 2011, **115**, 4425.

11 J. Jain, S. Arora, J. M. Rajwade, P. Omray, S. Khandelwal and K. M. Paknikar, *Mol.Pharm*., 2009, **6**, 1388; (b) Z. Mao, X. Zhoua and C. Gao, *Biomater. Sci*., 2013, **1**, 896.

12 J. J. Lin, W. C. Lin, R. X. Dong and S. H. Hsu, *Nanotechnology*, 2012, **23**, 065102; (b) T. Maneerunga, S. Tokurab and R. Rujiravanit, *Carbohydr. Polym*., 2008,**72**, 43; (c) V.R. Babu, C. Kim, S. Kim, C. Ahn and Y.I Lee, *Carbohydr. Polym*., 2010, **81**, 196

13 T. T. H. Anh, M. Xing, D. H. T. Le, A. Sugawara-Narutaki and E. Fong, *Nanomedicine*, 2013, **8**, 567.

14 J. M. Galloway and S. S. Staniland, *J. Mater. Chem*., 2012, **22**, 12423; (b) Y. Li, F. Zho, Y. Wen, K. Liu, L. Chen, Y. Mao, S. Yang and T. Yi, *Soft Matter*, 2014, **10**, 3077; (c) A. Shockravi, A. Jawadi and E.A. Lotf, *RSC Adv*., 2013, **3**, 6717.

15 M. J. Webber, J. Tongers, M. A. Renault, J. G. Roncalli, D. W. Losordo and S. I. Stupp, *Acta Biomater*., 2010, **6**, 3.

16 G. A. Silva, C. Czeisler, K. L. Niece, E. Beniash, D. A. Harrington and J. A. Kessler, *Science*, 2004, **303**, 1352.

17 J. B. Matson, R. H. Zha and S. I. Stupp, Curr. Opin. *Solid State Mater. Sci*., 2011, **15**, 225; (b) C. HeLary, A. Abed, G. Mosser, L. Louedec, D. Letourneur, T. Coradin, M.M.G. Guillea and A.M. Pelle, *Biomater. Sci*., 2015, **3**, 373

18 E. D. Spoerke, S. G. Anthony and S. I. Stupp, *Adv. Mater*., 2009, **21**, 425.

19 X. Zhao, F. Pan and J. R. Lu, Prog. Nat. Sci., 2008, **18**, 653; (b) M. Malmsten, *Soft Matter*, 2011, **7**, 8725.

20 X. Yan, P. Zhu and J. Li, *Chem. Soc. Rev*., 2010, **39**,1877.

21 Y. Pan, Y. Gao, J. Shi, L. Wang and B. Xu, *J. Mater. Chem*., 2011, **21**, 6804.

22 M. Zhang and B. C. Ye, *Anal. Chem*., 2011, **83**, 1504.

23 Z. Yang and B. Xu, *J. Mater. Chem*., 2007, **17**, 2385.

24 Z. Luo and S. Zhang, *Chem. Soc. Rev*., 2012, **41**, 4736.

25 Y. Kuang, Y. Gao and B. Xu, *Chem. Commun*., 2011, **47**, 12625.

26 X. Yan, F. Wang, B. Zheng and F. Huang, *Chem. Soc. Rev*., 2012, **41**, 6042.

27 J. F. Miravet and B. Escuder, *Chem. Commun*., 2005, **46**, 5796.

28 E. Cevher, D. Sensoy, M. A. M. Taha and A. Araman, *AAPS PharmSciTech*., 2008, **9**, 953.

29 S. K. Tripathy and Y. T. Yu, Spectrochim. *Acta Mol. Biomol. Spectros*., 2009, **72**, 841.

30 A. Ravindran, N. Chandrasekaran and A. Mukherjee, *Curr. Nanosci*., 2012, **8**, 141.

31 A. Shome, S. Dutta, S. Maiti and P. K. Das, *Soft Matter*, 2011, **7**, 3011.

32 X. Li, J. Zhang, W. Xu, H. Jia, X. Wang, B. Yang, B. Zhao, B. Li and Y. Ozaki, *Lgmuir*., 2003, **19**, 4285.

33 Z. M. Xiu, Q. B. Zhang, H. L. Puppala, V. L. Colvin and P. J. J. Alvarez, *Nano Lett*., 2012, **12**, 4271; (b) Y. Zhou, Y. Zhao, L. Wang, L. Xu, M. Zhai and S. Wei, *Radiat Phys Chem*., 2012, **81**, 553.

Table of Contents (TOC):

The Nap-FFC peptides through mineralization process produced transparent silver nanoparticle-based hydrogels (AgNPs@Nap-FFC) for antibacterial wound dressing.